Synthesis, radiolabeling and first biological characterization of ^{18}F-labeled xanthine derivatives for PET imaging of Eph receptors

Pretze, M.; Neuber, C.; Kinski, E.; Belter, B.; Köckerling, M.; Caflisch, A.; Steinbach, J.; Pietzsch, J.; Mamat, C.;

Originally published:

April 2020

Organic & Biomolecular Chemistry 18(2020)16, 3104-3116

DOI: https://doi.org/10.1039/D0OB00391C

Synthesis, radiolabeling and first biological characterization of ^{18}F-labeled xanthine derivatives for PET imaging of Eph receptors

Marc Pretze[a,b,‡,*], Christin Neuber[a,*], Elisa Kinski[a], Birgit Belter[a], Martin Köckerling[c], Amedeo Caflisch,[d] Jörg Steinbach[a,b], Jens Pietzsch[a,b], Constantin Mamat[a,b,**]

[a] Helmholtz-Zentrum Dresden-Rossendorf, Institut für Radiopharmazeutische Krebsforschung, Bautzner Landstraße 400, D-01328 Dresden, Germany
[b] Technische Universität Dresden, Fakultät Chemie und Lebensmittelchemie, D-01062 Dresden, Germany
[c] Universität Rostock, Institut für Chemie, Albert-Einstein-Straße 3a, D-18059 Rostock, Germany
[d] Department of Biochemistry, University of Zurich, Winterthurerstrasse 190, CH-8057 Zurich, Switzerland

* M.P. and C.N. contributed equally to this work.
[‡] current address: Klinik und Poliklinik für Nuklearmedizin, Universitätsklinikum Carl Gustav Carus der TU Dresden, Fetscherstraße 74, D-01307 Dresden, Germany

Abstract

Eph receptor tyrosine kinases, particulary EphA2 and EphB4, represent promising candidates for molecular imaging due to their essential role in cancer progression and therapy resistance. Xanthine derivatives were identified to be potent Eph receptor inhibitors with IC_{50} values in the low nanomolar range (1-40 nm).These compounds occupy the hydrophobic pocket of the ATP-binding site in the kinase domain. Based on lead compound **1**, we designed two fluorine-18-labeled receptor tyrosine kinase inhibitors (**[^{18}F]2/3**) as potential tracers for positron emission tomography (PET). Docking into the ATP-binding site allowed us to find the best position for radiolabeling. The replacement of the methyl group at the uracil residue (**[^{18}F]3**) rather than the methyl group of the phenoxy moiety (**[^{18}F]2**) by a fluoropropyl group was predicted to preserve the affinity of the lead compound **1**. Herein, we point out a synthesis route to **[^{18}F]2** and **[^{18}F]3** and the respective tosylate precursors as well as a labeling procedure to insert fluorine-18. After radiolabeling, both radiotracers were obtained in approximately 5% radiochemical yield with high radiochemical purity (>98%) and a molar activity of >10 GBq/µmol. In line with the docking studies, first cell experiments revealed specific, time-dependent binding and uptake of **[^{18}F]3** to EphA2 and EphB4 overexpressing A375 melanoma cells, whereas **[^{18}F]2** did not accumulate at these cells. Since both tracers **[^{18}F]3** and **[^{18}F]2** are stable in rat blood, the novel radiotracers might be suitable for in vivo molecular imaging of Eph receptors by, e.g., PET.

Introduction

The Eph (erythropoietin-producing hepatoma cell line) receptor family represents the largest subfamily of receptor tyrosine kinases and, at present, comprises 14 members divided into two groups, A and B. [1] Their corresponding, membrane-attached (GPI-anchored) ephrin A and (transmembrane located) ephrin B ligands bind to the Eph receptors in a juxtacrine manner which provides the condition for Eph receptor forward and ephrin reverse signaling. [2]
Eph receptors and their ephrin ligands play a crucial role during embryogenesis by regulating spatial patterning, vascular development, and axon guidance. [3, 4] Moreover, Eph/ephrin system is involved in tissue homoestasis, for instance of bone, intestine, and the immune system. [5, 6] All these effects are based on the regulation of cell–cell communication as well as cell attachment, shape, and motility by Eph receptors and their ephrin ligands.[7]

Beside their role during developmental processes it became evident that the Eph/ephrin system plays an important role in the pathogenesis of many diseases. [5] In this regard, Eph receptors are often dysregulated in cancer, whereby expression can be both up and down regulated.[8] Eph receptors can act both as tumor promotor and tumor suppressor, depending, e.g., on the cellular context, ligand stimulation, and the kind of resulting signaling crosstalk. [8, 9] In particular, EphA2 and EphB4 receptors are highly expressed in a number of tumor entities, including breast, prostate, lung, and ovarian cancer, and are often associated with poor prognosis [8, 10] as well as therapy resistance. [11, 12] Therefore, they are emerging targets for the functional characterization of tumors by noninvasive molecular imaging purposes like positron emission tomography (PET) or single photon emission computed tomography (SPECT), and the derivation of corresponding therapeutic applications.

In light of the involvement of the Eph/ephrin system in several pathologies including cancer, a wide range of agents targeting Eph receptors and their corresponding ephrins arose in the last years. To date, several potent Eph kinase inhibitors are reported in the literature either based on biomacromolecules like peptides[13],[14],[15], which bind to the extracellular ligand binding domain of the appropriate receptor, or based on small organic molecules,[16] which are able to block the intracellular ATP binding pocket. Selected compounds were chosen to be radiolabeled with either technetium-99m[17] for SPECT as well as with copper-64[18] or with fluorine-18[19] like peptide **I** [20] and small molecules with carbon-11 such as compound **IIIa** [21] for PET (Scheme 1).

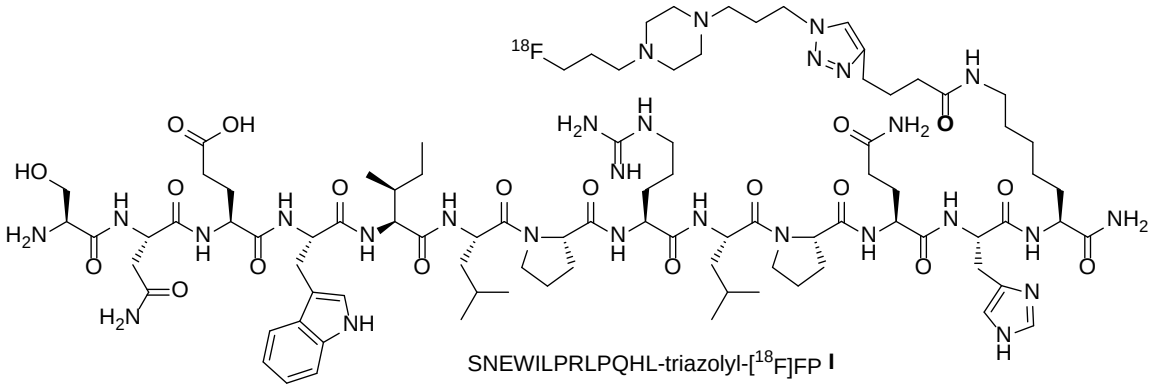

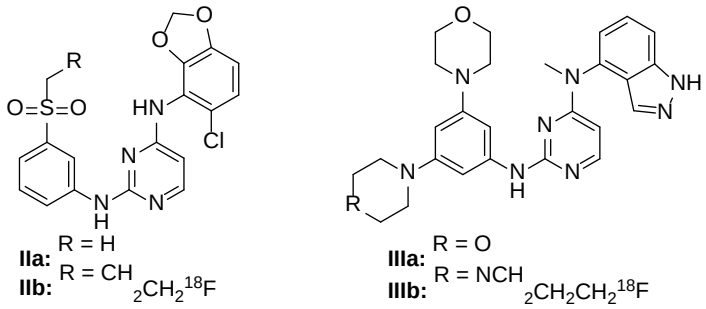

Scheme 1 Structures ^{11}C- and ^{18}F-labeled radiotracers **I**-**III** based on Eph inhibitors prepared by our group.

In the past, we developed the fluorine-18-containing radiotracers **IIb** [22] based on the benzodioxolylpyrimidine structural motif and **IIIb** [23] containing the indazolylpyrimidine core. Compound **IIb** showed a substantial uptake in human melanoma cells (A375) in vitro but no uptake in the corresponding melanoma xenograft model in vivo, despite of the high affinity of the original compounds to the EphB4 receptor. These results prompted us to search for an improved lead structure. In this regard, compound **1** (designated as compound **3** in [24]) containing a xanthine skeleton published by Nevado in 2009 and 2012 was chosen as lead compound.[24, 25] For lead compound **1**, a high affinity in the low nanomolar range (1-40 nm) was described for 10

Eph receptors including EphA2 and EphB4, the two receptors which are mainly involved in cancer progression and therapy resistance.
In the present paper, a synthesis route to two novel fluorine-18-containing derivatives (**[^{18}F]2/3**) of lead compound **1** and the respective precursors for radiolabeling as well as a labeling procedure to insert fluorine-18 is presented. Prior to synthesis and radiolabeling, in silico docking studies were accomplished to find the best position for labeling with fluorine-18. Based on these results first in vitro experiments were accomplished to investigate binding behavior to EphA2 and EphB4 overexpressing A375 melanoma cells and metabolic stability.

Results

In silico design

As most of the pharmaceuticals in clinical use do not contain fluorine, an isosteric radiolabeling with fluorine-18 is not possible if these molecules are also interesting for molecular imaging. Instead of this, single hydrogen atoms or functional groups like hydroxy groups are typically replaced by fluorine-18. [26] However, this replacement can lead to a change in the pharmacological behavior of the compounds. Thus, the search of an acceptable labeling position is mandatory and can be performed by docking studies, particularly, if the (holo) structure of the target protein has been reported.

The chosen lead compound **1**, containing a xanthine skeleton, has been published by the group of Nevado. [24] To investigate local selectivity (inhibitory activity on a single branch of the kinome dendrogram), lead compound **1** was tested by an enzymatic assay with [γ-^{33}P]ATP against a panel of 11 Eph receptor kinases. Due to the high sequence identity of Eph receptors (60-90%) and their small gatekeeper residue threonine in the ATP-binding site, compound **1** showed IC_{50} values in the nanomolar range for nearly all Eph receptors (IC_{50}: 2.9 nM (EphA1), 2.3 nM (EphA2), 3.3 nM (EphA4), 3.0 nM (EphA5), 4.5 nM (EphA8), 1.1 nM (EphB1), 1.2 nM (EphB2), 1.6 nM (EphB4)). [24] In general, the size of the gatekeeper residue of the hydrophobic pocket of the ATB binding site determines affinity as well as selectivity of RTK inhibitors.[27] Both EphA2 and EphB4 belong to the subfamily of kinases (~20% of the 518 human kinases) with a small (threonine) gatekeeper (Thr693). Moreover, compound **1** was tested for its global selectivity (inhibitory activity on the whole kinome) and was shown to strongly inhibit six further kinases (out of 85 tested), namely Src, Lck, Yes1, CSK, BTK, and HER-4, which all have a threonine gatekeeper.[24] Overall, lead compound **1** showed high inhibition against 21 out of 143 tested kinases, about half of which were chosen because of their small gatekeeper residue, and 10 of them are Eph kinases.

Explicit solvent molecular dynamics simulations of the complex of the kinase domain and a precursor of lead compound **1** (compound **3** in [24]), had revealed involvement of carbonyl C_6=O and amide group N_1-H in hydrogen bonds with the backbone polar groups of Met696 of EphB4. [24] For the development of the two novel ^{18}F-based radiotracers **[^{18}F]2** and **[^{18}F]3**, we decided to choose two sites of the original inhibitor that are not directly involved in binding interactions. Radiotracers **[^{18}F]2** and **[^{18}F]3** are based on the replacement of a methyl group by a fluoropropyl group at the phenoxy moiety and uracil residue of the lead compound **1**, respectively (Scheme 2). Starting from the crystal structure of compound **1** in the complex with the kinase domain (PDB code 4GK2), manual docking of the two derivatives was carried out with the program WITNOTP, which is available from the homepage of one of the authors (AC). The docking of inhibitor **2** resulted in steric clashes of the propyl chain with the N-terminal or C-terminal domain of the kinase depending on the orientation of the phenyl ring. In contrast, the fluorinated propyl of compound **3** could be accommodated without steric conflicts as it points towards the exposed region of the ATP binding site (Figure 1).

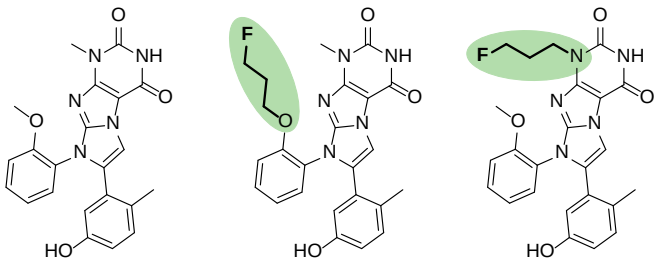

1 **2** **3**

Scheme 2 Literature known lead compound **1** and proposed structures of fluorine-containing-radiotracers **2** and **3** with highlighted labeling positions.

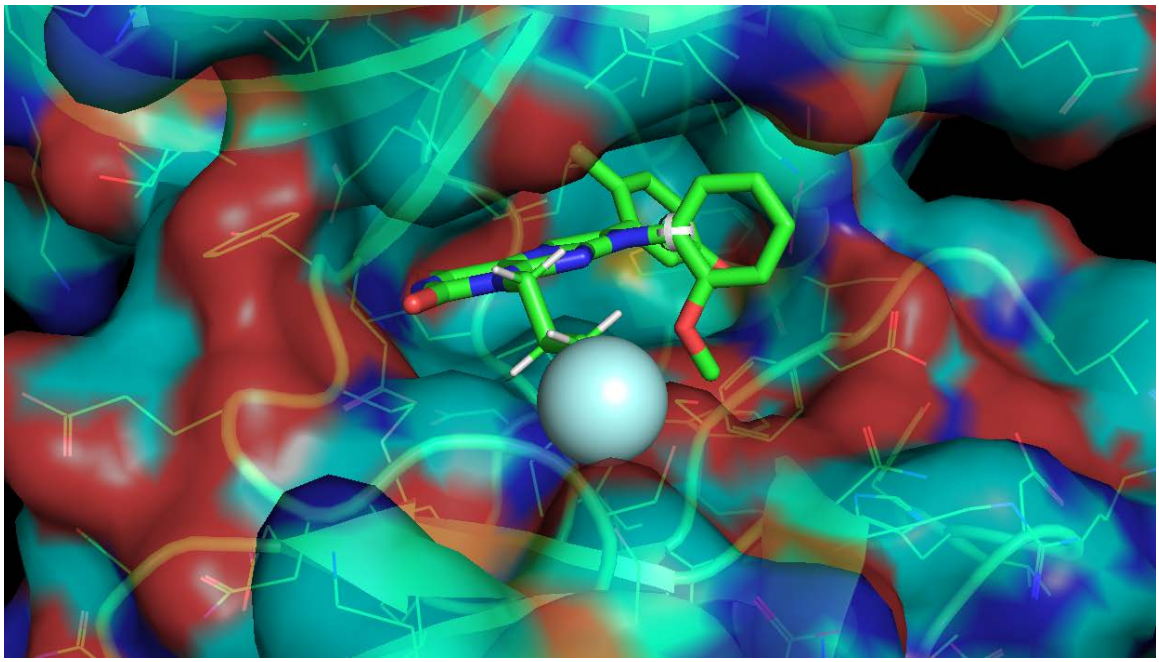

Figure 1 Predicted binding mode of compound **3** in the ATP binding site of the EphB4 receptor. The position of the fluorine atom is emphasized by a cyan sphere and hydrogen atoms are shown only for the propyl chain.

Chemistry

N-Modified aminouracils were applied as basis for the preparation of the original lead compound **1**, both ^{18}F-radiotracers **[^{18}F]2,3**, the non-radioactive reference compounds **2,3** and their respective precursors **14a,b**. In the first step, unsymmetrically alkylated urea derivatives **4a-c** were prepared from the respective amines and sodium cyanate. [28] Next, compounds **4a-c** were reacted with ethyl 2-cyanoacetate and sodium ethanolate in a Traube purin synthesis[29] to the *N*-substituted uracil derivatives **5a-c**. The preparation of the bromoxanthins was accomplished according to the literature. [24] For this purpose, all three uracil derivatives **5a–c** were treated with $NaNO_2$ under acidic conditions which resulted in the nitroso derivatives **6a–c** (yields: 79–83%). Next, the diamino compounds **7a–c** were prepared by the reduction of **6a–c** with sodium dithionite. Due to the instability of the free diamines, compounds **7a–c** were subsequently converted into the respective xanthines **8a-c** by treatment with triethyl orthoformiate and *p*-TsOH. The last step required the insertion of bromine. Therefore, **8a-c** were treated with elemental bromine for 3 h at 65°C. Bromo derivatives **9a-c** were obtained in high yields of 74–84%. The

whole reaction sequence to the brominated xanthines starting from the appropriate ureas is shown in Scheme 3.

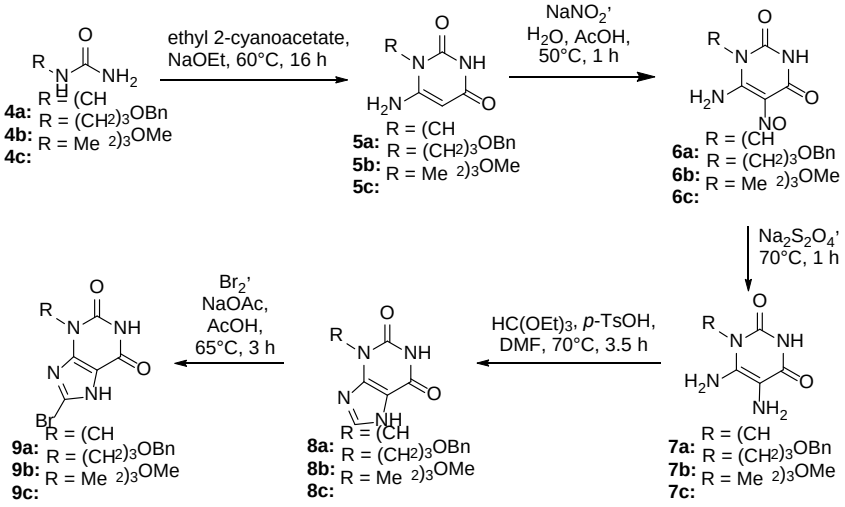

Scheme 3 Reaction sequence to brominated xanthine derivatives **9a-c** starting from urea derivatives **4a-c**.

During the synthesis of the urea derivatives **4a-c** and the bromo xanthines **9a-c**, it was possible to obtain single crystals of **4b** and **9a** suitable for single crystal X-ray analyses. The molecular structure of **4b** is presented in Figure 2 and that of **9a** in Figure 3.

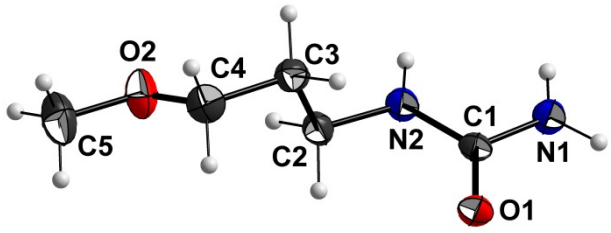

Figure 2 Molecular structure of **4b** in the crystal with atom labelling scheme (ORTEP plot, 50% probability level).

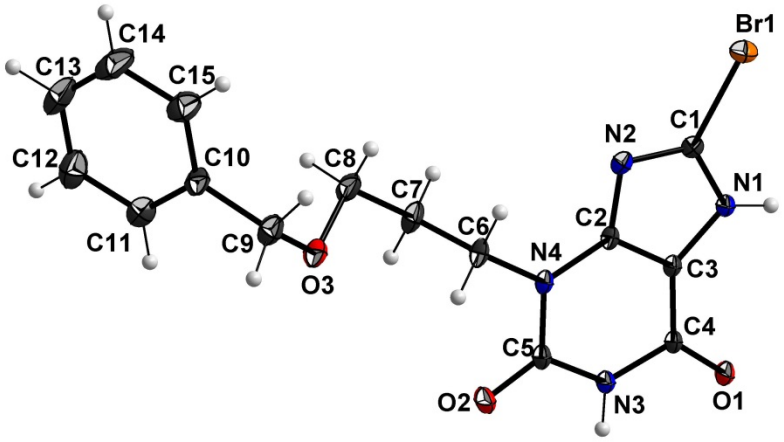

Figure 3 Molecular structure of **9a** in the crystal with atom labelling scheme (ORTEP plot, 50% probability level).

The compound **4b** crystallizes in the monoclinic and **9a** in the triclinic crystal system. The structures confirm the identities of the two compounds and the correctness of the reaction pathways. All bond distances in both structures are within the expected ranges. In crystals of **4b**, the molecules are arranged such that hydrogen bonds is formed between the NH_2 group (around N1) and the O1 atoms of neighboring molecules at distances of 2.927(1), 2.948(1), and 3.033(1) Å. In crystals of **9a** the molecules are arranged, such that the xanthine units as well as the phenyl rings of the benzyl group are arranged parallel to same units of neighboring molecules, but outside of distances of π-π-interactions. Hydrogen bonds exist between the H atoms of both NH groups (N1 and N3) to O1 and O2, respectively, of neighboring molecules at distances of 2.6875(9) and 2.817(1) Å.

The next reaction sequence to obtain the final compounds started with the synthesis of 2-bromo-1-(5-hydroxy-2-methylphenyl)ethanone (**10**),[24] which was then connected to xanthins **9a-c**. The desired compounds **11a-c** were obtained in nearly quantitative yields of >99%. At this stage, the benzyl group of **11a** as well as the methyl group of **11b** were inevitable to be cleaved with BBr_3 in dichloromethane to give **11d** (yield: 99% starting from **11a** and 84% starting from **11b**). The final cyclization reaction of **11c,d** with alkoxyanilines **12a,b** to the imidazopurinediones **13a-c** was accomplished under Lewis acid catalysis ($AlCl_3$), which is important for the success of the reaction. Otherwise, only open-chained products were obtained.[31] The synthesis was executed either with 2-methoxyaniline (**12a**) and **9c** to yield **13a** (62%) or with 2-(3-hydroxypropoxy)aniline (**12b**) and **11b** to give **13b** (83% yield). A further optimization consisted in the application of four equivalents of the respective aniline derivative (**12a** or **12b**). In addition, the original inhibitor **13c** was also obtained by the reaction of **11c** with 2-methoxyaniline (**12a**) in a yield of 88%. The full reaction sequence to the final compounds is shown in Scheme 4.

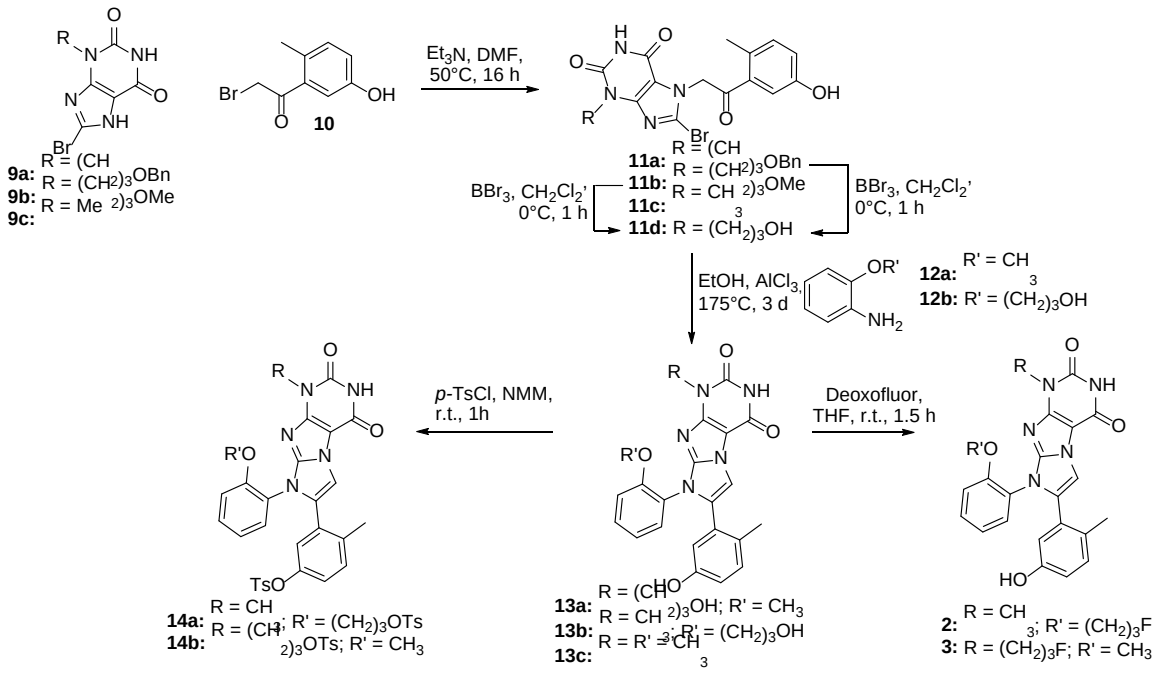

Scheme 4 Reaction sequence to the fluorinated reference compounds **2,3** and their tosylated precursors **14a,b**.

The last step to prepare the non-radioactive reference compounds **2** and **3** involved the introduction of fluorine into **13a,b**. Attempts to use **14a,b** for a nucleophilic introduction of fluoride were not successful. Alternatively, hydroxy compound **13a** was treated with deoxofluor in anhydrous THF under ambient temperature for 1 h which led to reference compound **3** in a yield of 10%. The second reference compound was synthesized from **13b** with DAST which led to **2** in a yield of 80%. Treatment of **13a,b** with *p*-TsCl in *N*-methylmorpholine yielded the desired precursors **14a** (96%) and **14b** (77%) for the later radiolabeling procedure. The use of DMF as solvent should be avoided due to the formation of unexpected by-products.[32]

logP determination

To give an impression of the later (radio-)pharmacological behavior of the radiofluorinated tracers, logP(D) values were calculated and compared with the experimentally determined values for the fluorinated compounds **2** and **3** as well as the lead compound **1** using ChemDraw and ACD labs (Table 1). Experimental determination using the shake flask method revealed suitable log P values of 2.2 for compound **2** and 2.9 of compound **3** which are comparable with the log P of the lead compound **1**.

Table 1 Calculated and determined log P(D) values for **2, 3**, and the lead compound **1**.

compound	lead compound **1**	**2**	**3**
calculated log P [33]	2.86	3.16	3.16
calculated log $D_{(pH\ 7.4)}$ [34]	1.67	2.24	2.29
determined log P	---	2.2	2.9

Radiolabeling

The radiosyntheses of both radiotracers **[^{18}F]2** and **[^{18}F]3** were achieved in a one-step procedure by classical aliphatic nucleophilic substitution of the tosylate group in precursors **14a,b** with n.c.a. [^{18}F]fluoride as shown in Scheme 5. Necessarily, the tosyl group attached to the phenyl moiety of **14a,b** has to be cleaved simultaneously. Labeling conditions were optimized for **[^{18}F]2** with regard to various reaction parameters such as solvent, reaction temperature, synthesis time and also in combination with microwave conditions. The resulting protocol was then transferred to the labeling procedure of **[^{18}F]3**.

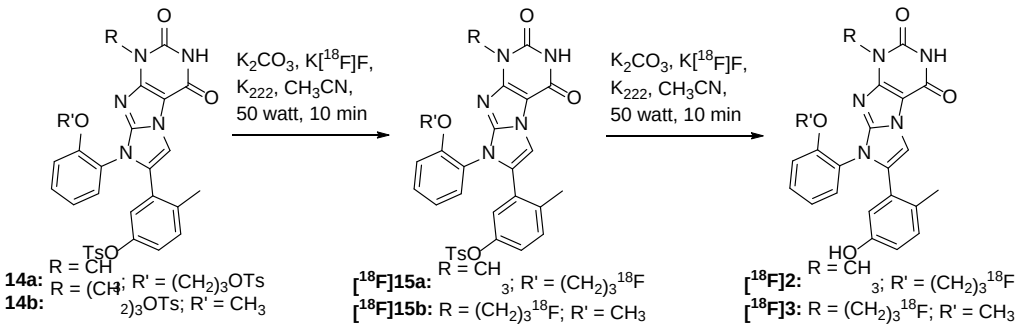

Scheme 5 Radiolabeling procedure for the synthesis of tracers **[^{18}F]2** and **[^{18}F]3**.

The use of [^{18}F]TBAF in *t*-butanol[35] and acetonitrile under standard heating and microwave conditions (15 and 30 W) for 10 min showed no conversion. When using 70 W for 10 min, a new spot was detected on the TLC with a R_f value of 0.55 (solvent: chloroform/MeOH = 9/1, silica gel), but not at the R_f value of the reference compound **2** (R_f = 0.37). The more lipophilic spot indicated the still tosyl group-containing tracer **[^{18}F]15a** of approx. 5%.
The use of K[^{18}F]F/K_{222}/K_2CO_3 mixture in acetonitrile at rt yielded the spot at R_f = 0.55 as well and a weak spot at R_f = 0.37. Finally, the use of mw conditions (10 min, 30 W) with the afore mentioned labeling conditions was successful and delivered a strong spot for the desired product at R_f = 0.37. An elongation of 40 min at 50 W delivered the tracer **[^{18}F]2** in 10% RCY and tosylated **[^{18}F]15a** in <2% RCY (Figure 4). Finally, after 70 min at 50 W only the desired product **[^{18}F]2** was detectable in 13% RCY (Scheme 5).

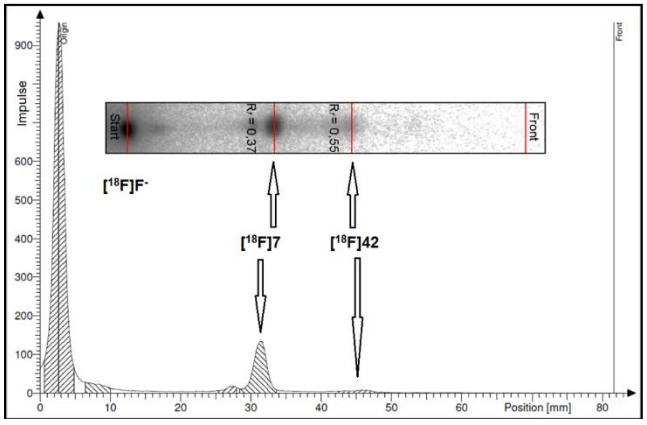

Figure 4 Radiolabeling of **[^{18}F]2**: Radio-TLC analysis (eluent: $CHCl_3$:MeOH 9:1), **[^{18}F]2** (R_f = 0.37) and **[^{18}F]15a** (R_f = 0.55) after 40 min at 50 watt.

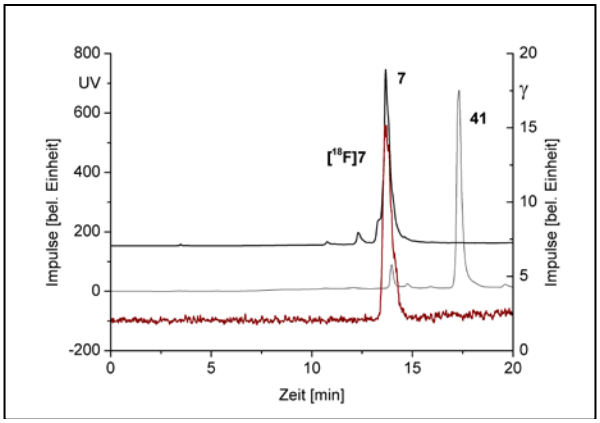

Figure 5 (radio-)HPLC chromatograms of purified **[^{18}F]2** (γ-trace: red line, t_R = 13.7 min), reference compound **2** (UV-trace: bold black line, t_R = 13.7 min) and precursor **41** (UV-trace: black line, t_R = 17.4 min).

The purification of **[^{18}F]2** was executed using two Chromafix® C18 cartridges. For this purpose, the reaction mixture was diluted with deionized water and the resulting solution was transferred to the cartridges. The first elution was done with deionized water to remove remaining [^{18}F]fluoride. The still trapped **[^{18}F]2** was eluted with MeOH and then finally purified using semipreparative HPLC to obtain 21–69 MBq (1 – 6 % d.c.) RCY with a A_m = 10.3 ± 5.1 GBq/µmol. Radio-TLC and radio-HPLC analyses showed no other radioactive by-products (Figure 5). Radiotracer **[^{18}F]3** was prepared via a two step procedure. First, the aliphatic OTs-group was converted under standard radiofluorination conditions using K_{222}, K_2CO_3 and [^{18}F]F^- at 100°C for 30 min. Afterwards, aqueous NaOH was added and the mixture was again heated at 100°C for 15 min to cleave the remaining aromatic tosyl group. Purification was done via semi-preparative HPLC to obtain **[^{18}F]3** in RCYs between 3–5%.

Radiobiological investigations

First, cellular binding and uptake of **[^{18}F]2** and **[^{18}F]3** was accomplished using A375 melanoma cells with low Eph receptor expression (A375) as well as in A375-EphA2 and A375-EphB4 cells, which are characterized by a substantial increased EphA2 and EphB4 expression, respectively (Figure 7A).

Cellular binding and uptake of radiotracer **[^{18}F]2** was lower than uptake of **[^{18}F]3** resulting in less and more than 50% ID/mg (injected dose per mg protein), respectively (Figure 7B/C). With regard to **[^{18}F]2** there was no difference in cellular tracer binding and uptake between non-transfected A375 cells and A375-EphA2 or A375-EphB4 cells (Figure 7B). The missing increase of tracer binding and uptake by time may result from (*i*) lack in Eph receptor affinity and/or (*ii*) active tracer efflux due to activity of multi drug resistance (MDR) proteins like P-glycoprotein (P-gp). With regard to the latter, Lafleur *et al.* already recognized that compound **1** is a substrate for P-gp transporters, since inhibitory activity of compound **1** decreased by almost two orders of magnitude when investigating IC_{50} in EphB4-overexpressing cells instead of by using recombinant protein (130 nm in cellular assay vs 5 nm in enzymatic assay) as a result of efficient substrate efflux. [25] In contrast to **[^{18}F]2**, cellular binding and uptake of **[^{18}F]3** was remarkably increased in A375-EphA2 and A375-EphB4 cells in comparison to A375 cells, amounting up to 110 and 90 % ID/mg, respectively (Figure 7C).

The specificity of radiotracer uptake was tested by performing blocking experiments with all three cell lines after pre-incubation with lead compound **1** or non-radioactive reference compound **2**. Cellular binding and uptake of **[^{18}F]2** in A375-EphA2 cells could be significantly blocked by pre-incubation with compound **2** (100 µM) at all investigated time points, whereas tracer accumulation in A375-EphB4 cells could be blocked only after 120 min (Figure 7D). Pre-incubation with lead compound **1** (50 µM) significantly decreased tracer accumulation in all three cell lines at 30, 60, and 120 min (Figure 7E). With regard to this, it has to keep in mind that lead compound **1** showed IC_{50} values in low nanomolar range (1-40 nm) against almost all Eph receptors due to their high sequence identity (60-90%) and their small gatekeeper residue (threonine) of the hydrophobic pocket of their ATP-binding site. [13] Since we could demonstrate mRNA expression of EphA1-4, EphA7, and EphB1-B4 in A375 cells in a previous study,[16] this might be the reason for the inhibition of radiotracer binding and uptake even in non-transfected A375 cells.

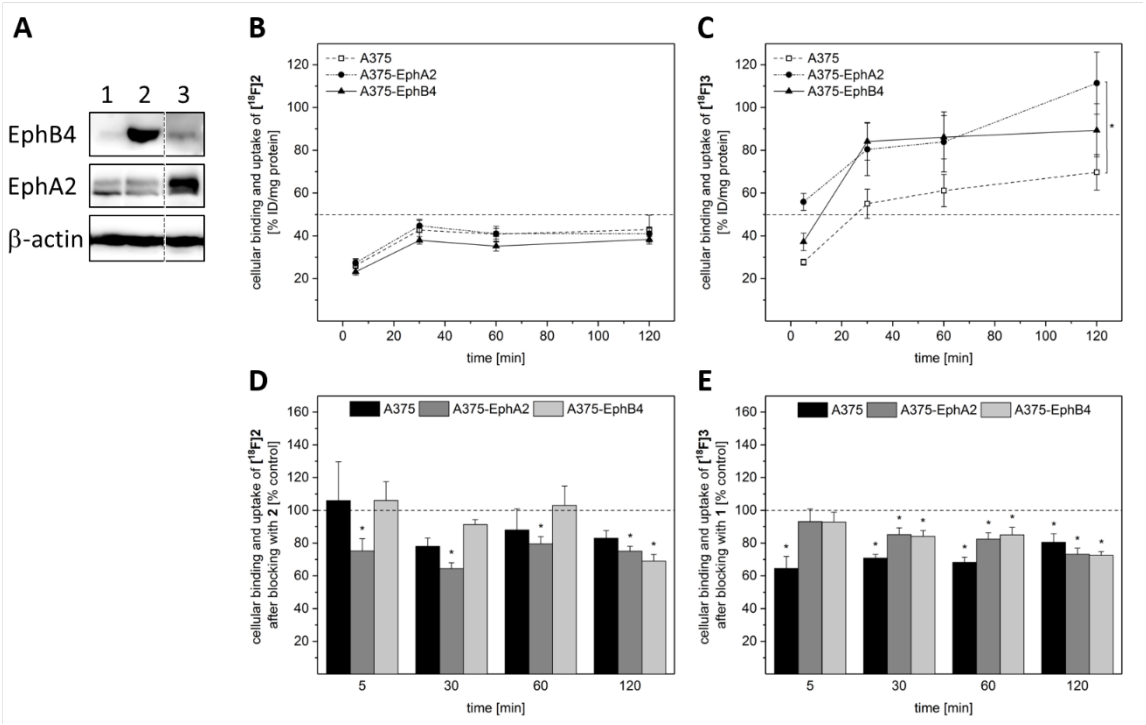

Figure 6 Cellular binding and uptake of radiotracer **[^{18}F]2** and **[^{18}F]3** over a period of 120 min at 37°C in non-transfected as well as EphA2- and EphB4-transfected A375 melanoma cells. (A) Representative western blots for EphA2 and EphB4 in (1) A375, (2) A375-EphB4, and (3) A375-EphA2 cells. (B/C) Cellular binding and uptake of radiotracers **[^{18}F]2** and **[^{18}F]3** in A375, A375-EphA2, and A375-EphB4 cells after 5, 30, 60, and 120 min at 37°C. (D/E) For blocking experiments, cellular binding and uptake of radiotracers **[^{18}F]2** and **[^{18}F]3** was investigated in all three cell lines after pre-incubation with compound **2** and lead compound **1**, respectively. Values represent mean ± standard deviation (SD) from at least two independent experiments each performed in quadruplicate.

Furthermore, first in vitro stability tests were accomplished with **[^{18}F]2** and **[^{18}F]3** in rat plasma and blood at 37°C up to 60 min via radio-TLC and radio-HPLC. No radiodefluorination or other degradation processes were observed for both **[^{18}F]2** and **[^{18}F]3** within at least 60 min. Further metabolite analyses using rats investigations using **[^{18}F]2** and **[^{18}F]3** after 60 min p.i. showed a fast blood clearance, no activity was found in the blood. In addition to that, a nearly complete degradation of **[^{18}F]2** and **[^{18}F]3** combined with the formation of a more hydrophilic metabolite in the urine was found.

Discussion

Due to promiscuity of the Eph receptor-Ephrin-system and missing selectivity of radiotracers targeting the hydrophobic pocket of the ATP-binding site[36, 37] we consciously decided to test a multi-Eph receptor tracer approach by choosing an imidazopurinedione derivative developed by Nevado/Lafleur (lead compound **1**) as lead compound for radiolabeling with fluorine-18. Due to the high sequence identity of Eph receptors (60-90%) and their small gatekeeper residue (threonine) in the hydrophobic pocket of the ATP-binding site, lead compound **1** showed IC_{50} values in low nanomolar range (1-40 nM) against EphA1-5, EphA8, and EphB1-4. For EphA2 and EphB4, which are mainly involved in cancer progression and therapy resistance, IC_{50} values in an enzymatic assay using [γ-^{33}P]ATP were 2.3 nM and 1.6 nM, respectively. Moreover, lead compound **1** was shown to strongly inhibit six further kinases (out of 85 tested), namely Src, Lck, Yes1, CSK, BTK, and HER-4, which all have a threonine gatekeeper. [24]

For purpose of nuclear imaging, especially by PET, we developed two derivatives of lead compound **1**, each bearing a [^{18}F]fluoropropyl side chain instead of a methyl group at the phenoxy ring (**[^{18}F]2**) and uracile (**[^{18}F]3**), respectively. Docking studies suggested a diminished binding

potential to EphB4 for **[^{18}F]2**. However, in vitro assay pointed out a high stability of **[^{18}F]2** in rat blood. In first cellular binding and uptake experiments, we could not observe a time-dependent increase in cellular binding and uptake of **[^{18}F]2** in EphA2 or EphB4 overexpressing A375 melanoma cells, which is in line with the docking prediction, but might also be the consequence of MDR protein, e.g., P-gp, mediated tracer efflux. Therefore, we focused on compound **[^{18}F]3**, bearing a [^{18}F]fluoropropyl side chain instead of a methyl group at the uracil residue. Docking experiments predicted a conserved binding affinity for this compound. In line with this, we found an increased cellular binding and uptake of **[^{18}F]3** to A375 melanoma cells overexpressing EphA2 or EphB4. Moreover, blocking with compound **1** revealed specificity of binding. Since this tracer was quite stable in rat blood in vitro over 60 min and, therefore, might be suitable for in vivo applications, future studies now have to focus on blood clearance rate and metabolic stability in vivo to finally assess feasibility of our newly developed radiotracer **[^{18}F]3** for in vivo molecular imaging, e.g. by PET.

Experimental Section

Chemistry

Instrumentation and chemicals: All reagents were purchased from commercial suppliers and were used without further purification. Compounds **4b-7b** were prepared according to van Muijlwijk-Koezen *et al.* [38] and compounds **4c-13c** were prepared according to Lafleuer *et al.* [24] Analytical TLC was performed on pre-coated Silica Gel 60 F_{254} plates (Merck) and results read under UV-light (λ = 254 nm). ^{1}H NMR, ^{13}C NMR and ^{19}F NMR spectra were recorded on a Varian Inova-400 or an Agilent 400-DD2 spectrometer with ProbeOne at 400, 101, and 376 MHz, respectively. Chemical shifts are reported in ppm with tetramethylsilane (^{1}H, ^{13}C) and trichlorofluoromethane (^{19}F) as internal standard, respectively. MS spectra were obtained on a Micromass Quattro-LC spectrometer using electron spray (ESI) as ionization method. Melting points were recorded on a Cambridge Instruments Galen III apparatus and are uncorrected. Single-crystal X-ray diffraction data of **4b** (CCDC 1976810) and **9a** (CCDC 1976126) were collected with a Bruker-Nonius Apex-X8 CCD-diffractometer using graphite-monochromated MoK_α radiation (λ = 0.71073 Å). The diffraction measurements were done at –150°C. The structures were solved by Direct Methods and refined against F^2 on all data by full-matrix least-squares using the SHELX suite of programs.[39] All non-hydrogen atoms were refined anisotropically; all hydrogen atoms bound to C atoms were placed on calculated positions and refined using a riding model. Final R values converged at R^1 = 0.035 (**4b**) and R^1 = 0.030 (**9a**). Analytical HPLC was performed on a VWR/Hitachi Elite La Chrome HPLC system, equipped with a reverse phase column (Nucleosil 100-5C18 Nautilus), a UV-diode array detector (254 nm) and a scintillation radiodetector (Raytest, Gabi Star) at a flow rate of 1 mL/min (eluent: acetonitrile/water, 30:70 + 0.1% TFA). The radioactive compound was identified using analytical radio-HPLC by comparison of the retention time t_R of the reference compound. Semi-preparative radio-HPLC was performed on a Jasco HPLC system (Nucleosil Standard C18 100Å 7µ, Macherey-Nagel, 250 x 16 mm, eluent: CH_3CN/H_2O + 0.1% TFA / 0 → 1 min: 90% H_2O, 1 → 18 min: 90% → 10% H_2O, 18 → 25 min: 10% H_2O, flow rate: 4 mL/min). Decay-corrected RCYs were quantified by integration of radioactive peaks on a radio-TLC using a radio-TLC scanner (Fuji, BAS2000). [^{18}F]Fluoride was produced by the ^{18}O(*p*,*n*)^{18}F nuclear reaction utilizing the PET cyclotron Cyclone 18/9 (IBA, Belgium) by irradiation of [^{18}O]H_2O.

1-(3-(Benzyloxy)propyl)urea (4a): Under Ar, 1-(3-(benzyloxy)propan-1-amine (2.35 g, 14.22 mmol) was dissolved in water (10 mL) and NaNCO (1.11g, 17.07 mmol) was added in five portions within 10 min. Afterwards, the mixture was heated at 100°C for 30 min, cooled to rt and was allowed to stand overnight. The precipitated product (scratch with glas rod) was filtered and washed with a small amount of cold water to give **4a** as colorless solid (1.10 g, 37%). Mp: 80–82°C; R_f = 0.44 (ethyl acetate:MeOH = 6:1). ^{1}H NMR (400 MHz, $CDCl_3$): δ = 7.40–7.27 (m, 5H, H_{Ar}), 4.99 (br s, 1H, NH), 4.61 (br s, 2H, NH_2), 4.49 (s, 2H, CH_2Ph), 3.58 (t, ^{3}J = 5.7 Hz, 2H, NCH_2), 3.28 (t, ^{3}J = 6.1 Hz, 2H, OCH_2), 1.83–1.77 (m, 2H, CH_2) ppm. ^{13}C NMR (101 MHz,

$CDCl_3$): δ = 158.8 (C=O), 138.1 (C-i), 128.5 (C-m), 127.8 (C-p), 127.7 (C-o), 73.1 (CH_2Ph), 68.5 (OCH_2), 38.8 (NCH_2), 29.7 (CH_2) ppm. MS (ESI+): *m/z* (%) = 231 (100) $[M + Na]^+$, 209 (35) $[M + H]^+$.

6-Amino-1-(3-(benzyloxy)propyl)pyrimidine-2,4(1*H*,3*H*)-dione (5a): Elemental sodium (1.86 g, 80.7 mmol) was dissolved in absolute EtOH (100 mL) and **4a** (5.6 g, 53.8 mmol) and ethyl cyanoacetate (6.09 g, 53.8 mmol) were added to this solution and the resulting mixture was heated to 60°C for 16 h. An organge precipitate appeared which disappeared after addition of conc. HCl to pH ≈ 3 under formation of a colorless precipitate. This was filtered and washed with EtOH (10 mL) and ethyl acetate (20 mL). The solvent was removed and the remaining residue was purified via column chromatography (ethyl acetate → ethyl acetate:EtOH = 10:1) and **5a** was obtained as bright yellow solid (3.8 g, 51%). Mp: 171–173°C; R_f = 0.30 (ethyl acetate:EtOH = 6:1). ^{1}H NMR (400 MHz, DMSO-d_6): δ = 10.30 (s, 1H, NH), 7.37–7.26 (m, 5H, H_{Ar}), 6.73 (s, 2H, NH_2), 4.53 (s, 1H, CH), 4.44 (s, 2H, CH_2Ph), 3.82 (t, ^3J = 7.3 Hz, 2H, NCH_2), 3.46 (t, ^3J = 6.3 Hz, 2H, OCH_2), 1.83–1.77 (m, 2H, CH_2). ^{13}C NMR (101 MHz, DMSO-d_6): δ = 162.2 (C=O), 155.6 (CNH_2), 151.1 (C=O), 138.3 (C-i), 128.1 (C-m), 127.4 (C-o), 127.3 (C-p), 75.4 (CH), 71.8 (CH_2Ph), 67.0 (OCH_2), 38.2 (NCH_2), 27.7 (CH_2). MS (ESI +): *m/z* (%) = 298 (40) $[M + Na]^+$, 276 (30) $[M + H]^+$.

6-Amino-1-(3-(benzyloxy)propyl)-5-nitrosopyrimidine-2,4(1*H*,3*H*)-dione (6a): Compound **5a** (1.46 g, 5.30 mmol) was suspended in a mixture of water (30 mL) and acetic acid (12 mL), $NaNO_2$ (548 mg, 7.96 mmol) was added and the mixture was maintained at 50°C for 1 h and at 4°C overnight. The resulting purple precipitate was filtered and washed with ice water. The resulting solid was dried at 80°C for 3 h and compound **6a** was obtained as deep purple solid (1.13 g, 70%). Mp.: 118–120°C, R_f = 0.34 (ethyl acetate:EtOH = 6:1). ^{1}H NMR (400 MHz, DMSO-d_6): δ = 13.34 (s, 1H, NH_2), 11.48 (s, 1H, NH), 9.06 (s,1H, NH_2), 7.35–7.25 (m, 5H, H_{Ar}), 4.42 (s, 2H, CH_2Ph), 3.88 (t, ^3J = 7.2 Hz, 2H, NCH_2), 3.48 (t, ^3J = 6.1 Hz, 2H, OCH_2), 1.83–1.77 (m, 2H, CH_2). ^{13}C NMR (101 MHz, DMSO-d_6): δ = 160.3 (C=O), 151.1 (CNH_2), 148.8 (C=O), 138.8 (CN=O), 138.3 (C-i), 128.2 (C-m), 127.5 (C-o), 127.4 (C-p), 71.9 (CH_2Ph), 67.1 (OCH_2), 38.1 (NCH_2), 26.5 (CH_2). MS (ESI +): *m/z* (%) = 327 (50) $[M + Na]^+$, 305 (100) $[M + H]^+$. MS (ESI –): *m/z* (%) = 303 (100) $[M – H]^-$.

5,6-Diamino-1-(3-(benzyloxy)propyl)pyrimidine-2,4(1*H*,3*H*)-dione hydrochloride (7a): Sodium dithionite (1.14 g, 5.57 mmol) was added portionwise to a suspension of **6a** (1.13 g, 3.71 mmol) in water (20 mL) and the resulting solution was heated at 70°C for 1 h (the color was turned to hight-green). Next, the volume of the solution was reduced by half and then cooled. The precipitate was filtered, washed with ice water and the resulting solid was dried at 90°C for 3 h and compound **7a** was obtained as light-green solid (1.12 g, 99%). Mp.: 261–262°C (decomp.), R_f = 0.14 (ethyl acetate:MeOH = 2:1). ^{1}H NMR (400 MHz, DMSO-d_6): δ = 10.53 (s, 1H, NH), 7.37–7.26 (m, 5H, H_{Ar}), 6.09 (s, 2H, NH_2), 4.45 (s, 2H, CH_2Ph), 3.86 (t, ^3J = 7.2 Hz, 2H, NCH_2), 3.47 (t, ^3J = 6.3 Hz, 2H, OCH_2), 2.83 (s, 2H, NH_2), 1.84–1.77 (m, 2H, CH_2) ppm. ^{13}C NMR (101 MHz, DMSO-d_6): δ = 159.6 (C=O), 149.3 (CNH_2), 145.4 (C=O), 138.4 (C_{ipso}), 128.2 (C_{meta}), 127.6 (C_{ortho}), 127.4 (C_{para}), 96.3 (NCC=O), 71.9 (CH_2Ph), 67.1 (OCH_2), 30.7 (NCH_2), 28.0 (CH_2). MS (ESI +): *m/z* (%) = 313 (20) $[M + Na]^+$, 291 (100) $[M + H]^+$. MS (ESI –): m/z (%) = 289 (40) $[M – H]^-$. Due to the instability of that compound, it should be immediately converted into its hydrochloride. Thus, the product (1.12 g) was treated with ice-cold HCl (37%, 15 mL) and stirred for 1h at rt. The HCl was removed under vacuum and the remaining solid dried under vacuum to yield the hydrochloride **7a** as hygroscopic pale red solid (1.27g, 99%). Mp.: 128–130°C (decomp.); R_f = 0 (ethyl acetate:MeOH = 2:1). ^{1}H NMR (400 MHz, DMSO-d_6): δ = 11.14 (s, 1H, NH), 9.31 (s, 3H, NH_3^+), 7.64 (s, 2H, NH_2), 7.37–7.26 (m, 5H, H_{Ar}), 4.44 (s, 2H, CH_2Ph), 3.91 (t, ^3J = 7.2 Hz, 2H, NCH_2), 3.48 (t, ^3J = 6.2 Hz, 2H, OCH_2), 1.84–1.77 (m, 2H, CH_2); ^{13}C NMR (101 MHz, DMSO-d_6): δ = 158.7 (C=O), 149.9 (CNH_2), 149.5 (C=O), 138.4 (C_{ipso}), 128.2 (C_{meta}), 127.5 (C_{ortho}), 127.4 (C_{para}), 83.0 (NCC=O), 71.9 (CH_2Ph), 67.0 (OCH_2), 39.5 (NCH_2), 27.6 (CH_2) ppm. MS (ESI +): *m/z* (%) = 313 (20) $[M + Na – HCl]^+$, 291 (100) $[M + H – HCl]^+$.

3-(3-(Benzyloxy)propyl)-1*H*-purine-2,6(3*H*,7*H*)-dione (8a): Compound **7a** (2.0 g, 6.12 mmol) was dissolved in anhydrous DMF (30 mL) under an argon atmosphere. Triethyl orthoformiate (2.29 mL, 13.77 mmol) and *p*-toluenesulfonic acid (monohydrate, 150 mg, 0.79 mmol) were added and the mixture was stirred at 70°C for 3.5 h. After cooling to rt, ice water (10 mL) was added and the mixture was allowed to crystallize at approx. 4°C overnight. Next, the solid was filtered and washed with cold water. After drying at 90°C, compound **8a** was obtained as yellowish solid (76%, 1.4 g). Mp.: 241–242°C, R_f = 0.51 (ethyl acetate:MeOH = 4:1). ^{1}H NMR (400 MHz, DMSO-d_6): δ = 13.47 (s, 1H, NHCH), 11.07 (s, 1H, NHC=O), 8.01 (s, 1H, CH), 7.35–7.25 (m, 5H, H_{Ar}), 4.41 (s, 2H, CH_2Ph), 4.03 (t, ^3J = 7.0 Hz, 2H, NCH_2), 3.49 (t, ^3J = 6.1 Hz, 2H, OCH_2), 1.97–1.90 (m, 2H, CH_2) ppm. ^{13}C NMR (101 MHz, DMSO-d_6): δ = 154.7 (C=O), 150.8 (C=O), 149.3 (CH), 140.5 (NCN), 138.5 (C-i), 128.2 (C-m), 127.4 (C-o), 127.3 (C-p), 106.9 (NCC=O), 71.9 (CH_2Ph), 67.4 (OCH_2), 39.8 (NCH_2), 27.9 (CH_2) ppm. MS (ESI +): *m/z* (%) = 323 (40) $[M + Na]^+$, 301 (100) $[M + H]^+$. MS (ESI –): *m/z* (%) = 299 (100) $[M – H]^–$.

3-(3-(Methyloxy)propyl)-1*H*-purine-2,6(3*H*,7*H*)-dione (8b): Compound **7b** (2.56 g, 10.2 mmol) was dissolved in anhydrous DMF (30 mL) under an argon atmosphere. Triethyl orthoformiate (3.66 mL, 22.0 mmol) and *p*-toluenesulfonic acid (monohydrate, 251 mg, 1.32 mmol) were added and the mixture was stirred at 70°C for 3.5 h. After cooling to rt, ice water (15 mL) was added and the mixture was allowed to crystallize at approx. 4°C overnight. Next, the solid was filtered and washed with cold water and acetone. After drying, compound **8b** was obtained as yellowish solid (55%, 1.25 g). Mp.: 221°C; ^{1}H NMR (400 MHz, DMSO-d_6): δ = 13.38 (s, 1H, NHCH), 11.03 (s, 1H, NHC=O), 7.98 (s, 1H, CH), 3.98 (t, ^3J = 7.2 Hz, 2H, NCH_2), 3.36 (t, ^3J = 6.2 Hz, 2H, OCH_2), 3.20 (s, 3H, CH_3), 1.83–1.91 (m, 2H, CH_2) ppm. ^{13}C NMR (101 MHz, DMSO-d_6): δ = 154.7 (C=O), 150.8 (C=O), 149.3 (CH), 140.6 (NCN), 107.2 (NCC=O), 69.5 (OCH_2), 57.8 (CH_3), 27.8 (CH_2) ppm. MS (ESI +): *m/z* (%) = 247 (40) $[M + Na]^+$, 225 (100) $[M + H]^+$.

3-(3-(Benzyloxy)propyl)-8-bromo-1*H*-purine-2,6(3*H*,7*H*)-dione (9a): Elemental bromine (144 µL, 2.83 mmol) was added dropwise to a solution of **8a** (710 mg, 2.36 mmol) and NaOAc (321 mg, 4.72 mmol) in glacial acetic acid (25 mL) and the resulting mixture was stirred at 65°C for 3 h. After cooling to 0°C, saturated bicarbonate solution (20 mL) was slowly added and the solution extracted with ethyl acetate (3 x 25 mL). The combined organic layers were dried over $MgSO_4$, the solvent was removed and the crude product was recrystalized with a small amount of dichloromethane to obtain **9a** as pale-yellow solid (750 mg, 84%). Mp.: 214–216°C, R_f = 0.64 (ethyl acetate:MeOH = 4:1). ^{1}H NMR (400 MHz, DMSO-d_6): δ = 11.16 (s, 1H, NHC=O), 7.35–7.26 (m, 5H, H_{Ar}), 4.41 (s, 2H, CH_2Ph), 3.97 (t, ^3J = 7.0 Hz, 2H, NCH_2), 3.48 (t, ^3J = 6.0 Hz, 2H, OCH_2), 1.95–1.90 (m, 2H, CH_2) ppm. ^{13}C NMR (101 MHz, DMSO-d_6): δ = 156.1 (C_{Br}), 154.3 (C=O), 151.1 (C=O), 139.1 (C-i), 128.8 (C-m), 128.1 (C-o), 128.0 (C-p), 80.0 (NCC=O), 79.3 (NCN), 72.6 (CH_2Ph), 68.0 (OCH_2), 39.9 (NCH_2), 28.4 (CH_2) ppm. MS (ESI +): *m/z* (%) = 403 (97) [M + Na, ^{81}Br]$^+$, 401 (100) [M + Na, ^{79}Br]$^+$, 381 (53) [M + H, ^{81}Br]$^+$, 379 (55) [M + H, ^{79}Br]$^+$. MS (ESI –): *m/z* (%) = 379 (100) [M - H, ^{81}Br]$^–$, 377 (97) [M - H, ^{79}Br]$^–$.

3-(3-(Methyloxy)propyl)-8-bromo-1*H*-purine-2,6(3*H*,7*H*)-dione (9b): Elemental bromine (360 µL, 7.08 mmol) was added dropwise to a solution of **8b** (1.25 g, 5.57 mmol) and NaOAc (750 mg, 9.14 mmol) in glacial acetic acid (25 mL) and the resulting mixture was stirred at 65°C for 3 h. After cooling to 0°C, saturated bicarbonate solution (20 mL) was slowly added and the solution extracted with ethyl acetate (3 x 25 mL). The combined organic layers were dried over $MgSO_4$, the solvent was removed and the crude product was recrystalized with a small amount of dichloromethane to obtain **9b** as pale-yellow solid (750 mg, 84%). H NMR (400 MHz, DMSO-d_6): δ = 11.17 (s, 1H, NHC=O), 3.92 (t, ^3J = 7.3 Hz, 2H, NCH_2), 3.35 (t, ^3J = 6.1 Hz, 2H, OCH_2), 3.19 (s, 3h, CH_3), 180–1.89 (m, 2H, CH_2); ^{13}C-NMR (101 MHz, DMSO-d_6): δ = 156.1 (C_{Br}), 154.3 (C=O), 151.1 (C=O), 139.1 (C-i), 128.8 (C-m), 128.1 (C-o), 128.0 (C-p), 80.0 (NCC=O), 79.3 (NCN), 72.6 (CH_2Ph), 68.0 (OCH_2), 39.9 (NCH_2), 27.7 (CH_2) ppm. MS (ESI +): *m/z* (%) = 327 (97) [M + Na, ^{81}Br]$^+$, 325 (100) [M + Na, ^{79}Br]$^+$, 305 (40) [M + H, ^{81}Br]$^+$, 303 (42) [M + H, ^{79}Br]$^+$.

3-(3-(Benzyloxy)propyl)-8-bromo-7-(2-(5-hydroxy-2-methylphenyl)-2-oxoethyl)-1*H*-purine-2,6(3*H*,7*H*)-dione (11a): Compound **9a** (930 mg, 2.45 mmol) and DIPEA (633 mg, 4.90 mmol)

were dissolved in anhydrous DMF (5 mL) and 2-bromo-1-(5-hydroxy-2-methylphenyl)ethanone (**10**, 843 mg, 3.68 mmol) dissolved in DMF (5 mL) was added dropwise and the resulting solution was stirred at 50°C overnight. Afterwards, the solvent was removed and the crude product was purified using column chromatography (chloroform → chloroform:MeOH = 25:1) to obtain **11a** as solid (1.3 g, 99%). Mp.: 172–173°C, R_f = 0.18 (ethyl acetate). ^{1}H NMR (400 MHz, DMSO-d_6): δ = 11.32 (s, 1H, NH), 9.74 (s, 1H, OH), 7.37–7.27 (m, 6H, H_{Ar}), 7.18 (d, $^3J_{3,4}$ = 8.3 Hz, 1H, H-3), 6.96 (dd, $^3J_{3,4}$ = 8.3 Hz, $^4J_{4,6}$ = 2.5 Hz, 1H, H-4), 5.70 (s, 2H, CH_2C=O), 4.43 (s, 2H, CH_2Ph), 4.02 (t, ^3J = 6.9 Hz, 2H, NCH_2), 3.51 (t, ^3J = 6.0 Hz, 2H, OCH_2), 2.29 (s, 3H, CH_3), 1.99–1.91 (m, 2H, CH_2) ppm. ^{13}C NMR (101 MHz, DMSO-d_6): δ = 194.1 (CH_2C=O), 155.4 (C-5), 154.1 (C=O), 150.2 (C=O), 148.7 (NCN), 138.4 (C-i), 134.6 (C-1), 133.0 (C-3), 129.2 (C-2), 128.2 (C-m), 128.0 (C_{Br}), 127.5 (C-o), 127.3 (C-p), 119.7 (C-4), 115.5 (C-6), 109.0 (NCC=O), 71.9 (CH_2Ph), 67.3 (OCH_2), 54.3 (CH_2C=O), 39.2 (NCH_2), 27.8 (CH_2), 19.7 (CH_3) ppm. MS (ESI +): *m/z* (%) = 551 (90) [M + Na, ^{81}Br]$^+$, 549 (100) [M + Na, ^{79}Br]$^+$, 527 (83) [M + H, ^{81}Br]$^+$, 529 (80) [M + H, ^{79}Br]$^+$.

3-(3-(Methyloxy)propyl)-8-bromo-7-(2-(5-hydroxy-2-methylphenyl)-2-oxoethyl)-1*H*-purine-2,6(3*H*,7*H*)-dione (11b): Compound **9b** (758 mg, 2.50 mmol) and DIPEA (485 mg, 3.75 mmol) were dissolved in anhydrous DMF (5 mL) and 2-bromo-1-(5-hydroxy-2-methylphenyl)ethanone (**10**, 630 mg, 2.75 mmol) dissolved in DMF (5 mL) was added dropwise and the resulting solution was stirred at 50°C overnight. Afterwards, the solvent was removed and the crude product was purified using column chromatography (chloroform → chloroform:MeOH = 20:1) to obtain **11b** as colorless solid (1.1 g, 97%). Mp.: 213°C, R_f = 0.38 (chloroform:MeOH = 9:1). ^{1}H NMR (400 MHz, DMSO-d_6): δ = 11.34 (s, 1H, NH), 9.75 (s, 1H, OH), 7.35 (d, $^3J_{4,6}$ = 2.3 Hz, 1H, H-6), 7.18 (d, $^3J_{3,4}$ = 8.4 Hz, 1H, H-3), 6.96 (dd, $^3J_{3,4}$ = 8.4 Hz, $^4J_{4,6}$ = 2.3 Hz, 1H, H-4), 5.71 (s, 2H, CH_2C=O), 3.97 (t, ^3J = 7.1 Hz, 2H, NCH_2), 3.39 (t, ^3J = 6.0 Hz, 2H, OCH_2), 3.22 (s, 3H, CH_3), 2.28 (s, 3H, CH_3), 1.86–1.92 (m, 2H, CH_2); ^{13}C NMR (101 MHz, DMSO-d_6): δ = 194.2 (CH_2C=O), 155.4 (C-5), 154.1 (C=O), 150.2 (C=O), 148.7 (NCN), 134.6 (C-1), 133.0 (C-3), 129.2 (C-2), 128.0 (C_{Br}), 119.7 (C-4), 115.5 (C-6), 109.0 (NCC=O), 69.5 (OCH_2), 57.9 (OCH_3), 54.3 (CH_2C=O), 39.8 (NCH_2), 27.7 (CH_2), 19.7 (CH_3) ppm. MS (ESI +): *m/z* (%) = 575 (85) [M + Na, ^{81}Br]$^+$, 573 (87) [M + Na, ^{79}Br]$^+$, 553 (23) [M + H, ^{81}Br]$^+$, 551 (25) [M + H, ^{79}Br]$^+$.

8-Bromo-7-(2-(5-hydroxy-2-methylphenyl)-2-oxoethyl)-3-(3-hydroxypropyl)-1*H*-purine-2,6(3*H*,7*H*)-dione (11d): Starting from **11a**: BBr_3 (1 M in CH_2Cl_2, 7.4 mL, 7.36 mmol) was slowly added to a suspension of **11a** (1.38 g, 2.64 mmol) in anhydrous CH_2Cl_2 (20 mL) at 0°C and the solution was stirred for 1 h at 0°C. Afterwrds, water was added for quenching and the formed precipitate was filtered, washed with CH_2Cl_2 (2 x 10 mL) and water (2 x 10 mL) and dried in vacuo to obtain **11d** as colorless solid (1.15 g, 99%). Starting from **11b**: BBr_3 (1 M in CH_2Cl_2, 7.0 mL, 9.96 mmol) was slowly added to a suspension of **11b** (1.0 g, 2.22 mmol) in anhydrous CH_2Cl_2 (20 mL) at 0°C and the solution was stirred for 1 h at 0°C. Afterwrds, water was added for quenching and the formed precipitate was filtered, washed with CH_2Cl_2 (2 x 10 mL) and water (2 x 10 mL) and dried in vacuo to obtain **9d** as colorless solid (813 mg, 84%). Mp.: 229–230°C, R_f = 0.50 (ethyl acetate:MeOH = 8:1). ^{1}H NMR (400 MHz, DMSO-d_6): δ = 11.33 (s, 1H, NH), 9.73 (s, 1H, HOPh), 7.35 (d, $^4J_{4,6}$ = 2.5 Hz, 1H, H-6), 7.18 (d, $^3J_{3,4}$ = 8.3 Hz, 1H, H-3), 6.96 (dd, $^3J_{3,4}$ = 8.3 Hz, $^4J_{4,6}$ = 2.5 Hz, 1H, H-4), 5.71 (s, 2H, CH_2C=O), 3.97 (t, ^3J = 7.5 Hz, 2H, NCH_2), 3.51 (t, ^3J = 6.4 Hz, 2H, OCH_2), 2.29 (s, 3H, CH_3) 1.85–1.78 (m, 2H, CH_2) ppm. ^{13}C NMR (101 MHz, DMSO-d_6): δ = 194.6 (CH_2C=O), 155.4 (C-5), 154.1 (C=O), 150.2 (C=O), 148.7 (NCN), 134.5 (C-1), 133.0 (C-3), 129.2 (C-2), 128.0 (C_{Br}), 119.7 (C-4), 115.5 (C-6), 109.0 (NCC=O), 58.5 (OCH_2), 54.3 (CH_2C=O), 38.7 (NCH_2), 31.0 (CH_2), 19.8 (CH_3) ppm. MS (ESI +): *m/z* (%) = 461 (25) [M + Na, ^{81}Br]$^+$, 459 (23) [M + Na, ^{79}Br]$^+$, 439 (100) [M + H, ^{81}Br]$^+$, 437 (97) [M + H, ^{79}Br]$^+$.

7-(5-Hydroxy-2-methylphenyl)-1-(3-hydroxypropyl)-8-(2-methoxyphenyl)-1*H*-imidazo[2,1-*f*]purine-2,4(3*H*,8*H*)-dione (13a): Compound **11d** (1.15 g, 2.64 mmol), 2-methoxyaniline (**12a**, 5.8 mL, 52.8 mmol) and $AlCl_3$ (anhydrous, 393 mg, 2.95 mmol) were dissolved in absolute EtOH (40 mL) and the mixture was heated at 175°C for 3 d in a high pressure reactor (quarz glass tube). Afterwards, the solvent was removed and the crude product was purified by column chromatography (ethyl acetate → ethyl acetate:MeOH 20:1) to obtain **13a** as a greyish solid (730 mg, 62%). Mp.: 282–283°C, R_f = 0.32 (ethyl acetate:MeOH = 10:1). ^{1}H NMR (400 MHz, DMSO-

d_6): δ = 10.97 (s, 1H, NH), 9.73 (s, 1H, HOPh), 7.74 (s, 1H, CH), 7.42–7.37 (m, 2H, H-4', H-6'), 7.12 (d, $^3J_{3,4}$ = 8.3 Hz, H-3), 7.00–6.97 (m, 2H, H-3',5'), 6.62 (dd, $^3J_{3,4}$ = 8.3 Hz, $^4J_{4,6}$ = 2.5 Hz, 1H, H-4), 6.55 (d, $^4J_{4,6}$ = 2.5 Hz, 1H, H-6), 4.45 (t, ^3J = 5.4 Hz, 1H, OH), 3.92 (t, ^3J = 7.1 Hz, 2H, NCH_2), 3.62 (s, 3H, OCH_3), 3.41 (dt, $^3J_{H,H}$ = 6.1 Hz, $^3J_{H,OH}$ = 5.4 Hz, 2H, $HOCH_2$), 2.11 (s, 3H, CH_3), 1.80–1.74 (m, 2H, CH_2) ppm. ^{13}C NMR (101 MHz, DMSO-d_6): δ = 154.7 (C-2'), 154.5 (C=O), 153.4 (C-5), 152.4 (C_q), 150.8 (C=O), 147.3 (NCN), 131.8 (C=CPh), 130.9 (C-3), 130.8 (C-4'), 129.5 (C-5'), 127.8 (C-1), 127.7 (C-1'), 122.3 (C-2), 120.7 (C-6'), 117.9 (C-4), 116.3 (C-3'), 112.8 (C-6), 106.3 (CH), 99.1 (NCC=O), 58.4 (OCH_2), 55.6 (OCH_3), 38.7 (NCH_2), 30.9 (-CH_2-), 18.7 (CH_3) ppm. MS (ESI +): *m/z* (%) = 484 (100) $[M + Na]^+$, 462 (45) $[M + H]^+$.

7-(5-Hydroxy-2-methylphenyl)-8-(2-(3-hydroxypropoxy)phenyl)-1-methyl-1*H*-imidazo[2,1-*f*]purine-2,4(3*H*,8*H*)-dione (13b): Compound **11c** (500 mg, 1.27 mmol), 2-(3-hydroxy(propoxy))aniline (**12b**, 1.81 g, 10.82 mmol) and $AlCl_3$ (anhydrous, 393 mg, 2.95 mmol) were dissolved in absolute EtOH (20 mL) and the mixture was heated at 175°C for 3 d in a high pressure reactor (quarz glass tube). Afterwards, the solvent was removed and the crude product was purified by column chromatography ($CHCl_3$:EtOH 15:1). Afterwards, the resulting solid was washed with ethyl acetate to obtain **13b** as a greyish solid (326 mg, 56%). R_f = 0.45 ($CHCl_3$:MeOH = 5:1). ^{1}H NMR (400 MHz, DMSO-d_6): δ =10.97 (s, 1H, 1-NH), 9.25 (s, 1H, PhOH), 7.74 (s, 1H, CH), 7.39 (dt, ^3J = 8.0 Hz, ^4J = 1.7 Hz, 1H, H-4'), 7.32 (dd, ^3J = 7.7 Hz, ^4J = 1.7 Hz, 1H, H-6'), 7.14 (dd, ^3J = 8.5 Hz, ^4J = 1.2 Hz, 1H, H-3'), 6.95–6.99 (m, 2H, H-3,H-5'), 6.63 (dd, $^3J_{3,4}$ = 8.3 Hz, $^4J_{4,6}$ = 2.6 Hz, 1H, H-4), 6.59 (d, $^4J_{4,6}$ = 2.6 Hz, 1H, H-6), 4.41 (t, ^3J = 5.1 Hz, 1H, OH), 3.91–4.04 (m, 2H, OCH_2), 3.28–3.34 (m, 5H, CH_2OH, NCH_3), 2.10 (s, 3H, $PhCH_3$), 1.71–1.61 (m, 2H, CH_2) ppm. ^{13}C NMR (101 MHz, DMSO-d_6): δ = 154.6 (C_q), 154.2 (C=O), 153.4 (Cq), 153.0 (C_q), 151.1 (C=O), 147.6 (NCN), 131.8 (C-1), 130.9 (C-3), 130.8 (C-4'), 129.7 (C-6'), 127.8 (C_q), 127.6 (C_q), 122.4 (C_q), 120.4 (C_q), 117.9 (C-6), 116.3 (C-4), 113.3 (C-3'), 106.4 (CH_{Hetar}), 99.1 (NCC=O), 65.3 (OCH_2), 57.1 (CH_2OH), 31.8 (-CH_2-), 28.8, 18.8 (2 x CH_3). MS (ESI +): *m/z* (%) = 484 (100) $[M + Na]^+$, 462 (60) $[M + H]^+$.

4-Methyl-3-(1-methyl-2,4-dioxo-8-(2-(3-(tosyloxy)propoxy)phenyl)-2,3,4,8-tetrahydro-1*H*-imidazo[2,1-*f*]purin-7-yl)phenyl 4-methylbenzenesulfonate (14a): Compound **13b** (250 mg, 0.54 mmol) was dissolved in anhydrous NMM (5 mL), tosyl chloride (437 mg, 2.29 mmol) was added and the mixture was allowed to stirr at rt overnight. Water was added to the reaction mixture, the precipitate was filtered off and purified via column chromatography (petroleum ether:ethyl acetate 1:5) to obtain **14a** as a pale yellow solid (400 mg, 96%). R_f = 0.79 ($CHCl_3$:MeOH = 10:1). ^{1}H NMR (400 MHz, DMSO-d_6): δ =11.01 (s, 1H, NH), 7.82 (s, 1H, CH), 7.62 (d, ^3J = 8.3 Hz, 2H, Ts-H_{ortho}), 7.51 (d, ^3J = 8.5 Hz, 2H, Ts-H_{ortho}), 7.45–7.35 (m, 4, Ts-H_{meta}), 7.39 (d, ^3J = 8.0 Hz, 2H, PhOTs-H_{meta}), 7.32 (d, ^3J = 8.1 Hz, 2H, H_{meta}), 7.14 (dd, ^3J = 7.9 Hz, ^4J = 1.5 Hz, 1H, H-3'), 7.16–7.08 (m, 2H, H-3',5'), 6.97-6.99 (m, 2H, H-3,H-6), 6.77 (dd, $^3J_{3,4}$ = 8.3 Hz, $^4J_{4,6}$ = 2.5 Hz, 1H, H-4), 3.99–3.86 (m, 4H, OCH_2+NCH_2), 3.29 (s, 3H, NCH_3), 2.41 (s, 3H, Me_{Ts}), 2.36 (s, 3H, Me_{Ts}), 2.11 (s, 3H, CH_3), 1.91–1.68 (m, 2H, CH_2) ppm. ^{13}C NMR (101 MHz, DMSO-d_6): δ = 153.7, 153.5, 152.9, 151.1, 147.5, 146.4, 145.8, 144.8, 137.3, 132.4 (2 x C=O + 8 x C_{Ar}), 131.5, 131.0 (2 x CH_{Ar}), 130.9 (CH_{Ar}), 130.1, 130.0 (2 x Ts-m), 129.8 (C_{Ar}), 129.6 (CH_{Ar}), 128.6 (C_{Ar}), 128.2 , 127.2 (2 x Ts-o), 113.5 (C-6), 107.2 (CH), 99.2 (NCC=O), 67.6, 63.9 (CH_2), 28.8 (NCH_3), 28.0 (CH_2), 21.1, 21.0 (2 x $TsCH_3$), 19.0 (CH_3) ppm. MS (ESI +): *m/z* (%) = 770 (90) $[M + H]^+$, 598 (15) $[M - OTs]^+$.

3-(8-(2-Methoxyphenyl)-2,4-dioxo-1-(3-(tosyloxy)propyl)-2,3,4,8-tetrahydro-1*H*-imidazo[2,1-*f*]purin-7-yl)-4-methylphenyl 4-methylbenzenesulfonate (14b): Compound **13a** (200 mg, 0.44 mmol) was dissolved in anhydrous NMM (5 mL), tosyl chloride (350 mg, 1.84 mmol) was added and the mixture was allowed to stirr at rt overnight. Water was added to the reaction mixture, the precipitate was filtered off and purified via column chromatography (petroleum ether:ethyl acetate 1:5) to obtain **14b** as a pale yellow solid (260 mg, 77%). Mp.: 89-90°C, R_f = 0.71 ($CHCl_3$:MeOH = 10:1). ^{1}H NMR (400 MHz, DMSO-d_6): δ = 10.95 (s, 1H, NH), 7.79 (s, 1H, CH), 7.64 (d, ^3J = 8.3 Hz, 2H, H_{ortho}), 7.48 (d, ^3J = 8.4 Hz, 2H, PhOTs-H_{ortho}), 7.46–7.43 (m, 1H, H-6'), 7.39 (d, ^3J = 8.0 Hz, 2H, PhOTs-H_{meta}), 7.32 (d, ^3J = 8.1 Hz, 2H, H_{meta}), 7.31–7.29 (m, 1H, H-4'), 7.16–7.10 (m, 2H, H-3',5'), 6.98 (dt, $^3J_{3,4}$ = 8.0 Hz, $^5J_{3,6}$ = 0.9 Hz, H-3), 6.88 (d, $^3J_{4,6}$ = 2.6 Hz, 1H, H-6), 6.73 (dd,

$^3J_{3,4}$ = 8.0 Hz, $^4J_{4,6}$ = 2.6 Hz, 1H, H-4), 4.01 (t, ^3J = 6.3 Hz, 1H, $TsOCH_2$), 3.83 (t, ^3J = 6.5 Hz, 2H, NCH_2), 3.54 (s, 3H, OCH_3), 2.36 (s, 3H, PhOTs-CH_3), 2.35 (s, 3H, $TsCH_3$), 2.18 (s, 3H, CH_3), 1.93–1.90 (m, 2H, CH_2) ppm. ^{13}C NMR (101 MHz, CD_3CN): δ = 156.0 (C-2'), 154.2 (C=O), 154.0 (C-5), 151.9 ($C(N)_3$), 148.9 (C=O), 147.9 (NCN), 147.3 ($PhTsO_{para}$), 146.3 (TsO_{para}), 138.9 (C-1), 132.6 (C=CPh), 132.3 ($PhTsO_{ipso}$, TsO_{ipso}), 131.6 (C-3), 131.0 ($PhTsO_{meta}$), 130.9 (TsO_{meta}), 130.5 (C-5'), 130.0 (C-2), 129.3 ($PhTsO_{ortho}$), 129.2 (C-4'), 128.6 (TsO_{ortho}), 126.6 (C-5'), 125.9 (C-1'), 124.0 (C-4), 123.2 (C-6'), 121.8 (C-3'), 113.7 (C-6), 107.9 (CH), 100.6 (NCC=O), 69.6 (OCH_2), 56.4 (OCH_3), 40.3 (NCH_2), 28.2 (NCH_2CH_2), 21.7 ($TsOCH_3$), 19.8 (CH_3) ppm. MS (ESI +): *m/z* (%) = 770 (90) $[M + H]^+$, 598 (15) $[M - OTs]^+$.

1-(3-Fluoropropyl)-7-(5-hydroxy-2-methylphenyl)-8-(2-methoxyphenyl)-1*H*-imidazo[2,1-*f*]purine-2,4(3*H*,8*H*)-dione (3): Compound **13a** (150 mg, 0.33 mmol) was dissolved in a mixtrue of NMM (5 mL) and DCM (5 mL). The reaction mixture was cooled to -78°C and DAST (200 µL, 1.51 mmol) was added stepwise. After complete addition the reaction mixture was stirred at rt overnight. Afterwards, ice was added, and the aqueous phase extracted with $CHCl_3$ (3 x 20 mL). The combined organic layers were washed with satturated hydrogen carbonate solution (20 mL) and water (20 mL). The crude product was purified by column chromatography ($CHCl_3$ → $CHCl_3$:MeOH 30:1 → 20:1 → 10:1) to obtain 3 as pale yellow solid (30 mg, 10%). Mp.: 194–195°C, R_f = 0.37 ($CHCl_3$:MeOH = 9:1). ^{1}H NMR (400 MHz, DMSO-d_6): δ = 9.23 (s, 1H, HOPh), 7.74 (s, 1H, CH), 7.41–7.37 (m, 2H, H-4',6'), 7.12 (dd, $^3J_{3,4}$ = 8.0 Hz, $^4J_{3,6}$ = 1.7 Hz, 1H, H-3), 7.02–6.97 (m, 2H, H-3',5'), 6.61 (dd, $^3J_{3,4}$ = 8.0 Hz, $^4J_{4,6}$ = 2.7 Hz, 1H, H-4), 6.54 (d, $^4J_{4,6}$ = 2.7 Hz, 1H, H-6), 4.48 (dt, $^3J_{H,F}$ = 47.3 Hz, $^3J_{H,H}$ = 5.8 Hz, 2H, FCH_2), 3.96 (t, ^3J = 6.2 Hz, 2H, NCH_2), 3.64 (s, 3H, OCH_3), 2.11 (s, 3H, CH_3), 1.94–1.93 (m, 2H, CH_2) ppm. ^{13}C NMR (101 MHz, DMSO-d_6): δ = 154.7 (C_q), 154.5 (C=O), 153.5 (C_q), 152.3 (C_q), 150.8 (C=O), 147.3 (NCN), 131.8 (C-1), 130.8 (C-3), 130.7 (C-4'), 129.5 (C-6'), 127.9 (C_q), 127.7 (C_q), 122.3 (C_q), 120.7 (C_q), 117.9 (C-6), 116.3 (C-4), 112.8 (C-3'), 106.3 (CH_{Hetar}), 99.2 (NCC=O), 79.5 ($^1J_{C,F}$ = 163.1 Hz, CH_2F), 63.8 ($^3J_{C,F}$ = 5.8 Hz, OCH_2), 29.5 (d, $^2J_{C,F}$ = 19.5 Hz, CH_2), 30.8, 18.7 (2 x CH_3). ppm. ^{19}F NMR (376 MHz, DMSO-d_6): = –218.3 ppm. MS (ESI +): *m/z* (%) = 464 (10) $[M + H]^+$. MS (ESI –): *m/z* (%) = 462 $[M – H]^–$.

8-(2-(3-Fluoropropoxy)phenyl)-7-(5-hydroxy-2-methylphenyl)-1-methyl-1*H*-imidazo[2,1-*f*]purine-2,4(3*H*,8*H*)-dione (2): Compound **13b** (100 mg, 0.22 mmol) was suspended in anhydrous THF (5 mL) and Deoxofluor (300 µL, 1.6 mmol) was added. After stirring at rt for 1.5 h, water (25 mL) was added and the aqueous solution extracted with ethyl acetate (3 x 20 mL). The crude product was purified by column chromatography (CH_2Cl_2:EtOH = 30:1) to give **1b** as a greyish solid (80 mg, 80%). Mp.: 308°C, R_f = 0.60 ($CHCl_3$:EtOH = 5:1). ^{1}H NMR (400 MHz, DMSO-d_6): δ = 10.99 (s, 1H, NH), 9.27 (s, 1H, HOPh), 7.76 (s, 1H, CH), 7.40 (dt, ^3J = 7.9 Hz, ^4J = 1.6 Hz, 1H, H-4'), 7.30 (dd, ^3J = 7.8 Hz, ^4J = 1.6 Hz, 1H, H-6'), 7.19 (dd, ^3J = 8.5 Hz, ^4J = 1.1 Hz, 1H, H-3'), 6.96–7.00 (m, 2H, H-3,H-5'), 6.64 (dd, $^3J_{3,4}$ = 8.3 Hz, $^4J_{4,6}$ = 2.6 Hz, 1H, H-4), 6.59 (d, $^4J_{4,6}$ = 2.6 Hz, 1H, H-6), 4.39–4.28 (m, 2H, CH_2F), 3.98–4.09 (m, 2H, OCH_2), 3.32 (s, 3H, NCH_3), 2.09 (s, 3H, $PhCH_3$), 2.00–1.81 (m, 2H, CH_2) ppm. ^{13}C NMR (101 MHz, DMSO-d_6): δ = 154.6 (C_q), 153.9 (C=O), 153.4 (C_q), 152.8 (C_q), 151.0 (C=O), 147.5 (NCN), 131.7 (C-1), 130.9 (C-3), 130.8 (C-4'), 129.7 (C-6'), 127.8 (C_q), 127.6 (C_q), 122.5 (C_q), 120.7 (C_q), 117.9 (C-6), 116.3 (C-4), 113.4 (C-3'), 106.5 (CH_{Hetar}), 99.1 (NCC=O), 80.4 ($^1J_{C,F}$ = 162.4 Hz, CH_2F), 64.0 ($^3J_{C,F}$ = 5.5 Hz, OCH_2), 29.5 (d, $^2J_{C,F}$ = 19.5 Hz, CH_2), 28.8, 18.7 (2 x CH_3) ppm. ^{19}F NMR (376 MHz, DMSO-d_6): = –220.7 ppm. MS (ESI +): *m/z* (%) = 486 (100) $[M + Na]^+$, 464 (30) $[M + H]^+$.

1-(3-[^{18}F]Fluoropropyl)-7-(5-hydroxy-2-methylphenyl)-8-(2-methoxyphenyl)-1*H*-imidazo[2,1-*f*]purine-2,4(3*H*,8*H*)-dione ([^{18}F]3): An anion-exchange cartridge (Waters, Sep-Pak Light Accell Plus QMA) was activated by rinsing with 5 mL of a 1 M $NaHCO_3$ solution and 10 mL of deionized H_2O. It was charged with [^{18}F]fluoride (~2 GBq) and eluted with 1.5 mL of a solution of Kryptofix 2.2.2 (10 mg/mL) and K_2CO_3 (13 mM) in 7 mL CH_3CN and 43 mL H_2O. The solvents were evaporated azeotropically by subsequent addition of three portions of 1 mL each of anhydrous CH_3CN under a stream of nitrogen at 110°C. Precursor **14b** (approx. 3 mg) was dissolved in 300 µL of anhydrous CH_3CN and the the mixture was added to the [^{18}F]fluoride-containing sealed vial. The resulting solution was heated under microwave conditions at 50 watt for 70 min. After cooling

to rt, 3 mL of water were added and the solution transferred to 2 connected Chromafix C18 ec-cartridges. The cartridges were washed with 20 mL of water and the tracer eluted with 0.9 mL of MeOH. Further purification was done via semi-preparative radio-HPLC (peak collection t_R: 9-11 min). To remove the solvent from the product, the solvent of the collected product fraction was removed under reduced pressure. Analytical radio-HPLC: t_R = 15.2 min; RCY: 21–69 MBq (1–6%, d.c.); RCP: > 98%; A_m = 10.3 ± 5.1 GBq/µmol.

8-(2-(3-[^{18}F]Fluoropropoxy)phenyl)-7-(5-hydroxy-2-methylphenyl)-1-methyl-1*H*-imidazo[2,1-*f*]purine-2,4(3*H*,8*H*)-dione ([^{18}F]2):An anion-exchange cartridge (Waters, Sep-Pak Light Accell Plus QMA) was activated by rinsing with 5 mL of a 1 M $NaHCO_3$ solution and 10 mL of deionized H_2O. It was charged with [^{18}F]fluoride (2–3 GBq) and eluted with 1.5 mL of a solution of Kryptofix 2.2.2 (10 mg/mL) and K_2CO_3 (13 mM) in 7 mL CH_3CN and 43 mL H_2O. The solvents were evaporated azeotropically by subsequent addition of three portions of 1 mL each of anhydrous CH_3CN under a stream of nitrogen at 110°C. Precursor **14a** (approx. 3 mg) was dissolved in 500 µL of anhydrous CH_3CN and the the mixture was added to the [^{18}F]fluoride-containing sealed vial. The resulting solution was heated at 100°C for 30 min. Afterwards, aqueous NaOH (40 µL, 5 M) was added and the mixture heated at 100°C for 15 min. After cooling to rt, 120 µL of water were added and the solution purified by semi-preparative radio-HPLC (peak collection t_R: 24–28 min, gradient: 60% water, 40% CH_3CN + 0.1% TFA). To remove the solvent from the product, the solvent of the collected product fraction was removed under reduced pressure. Analytical radio-HPLC: t_R = 12.0 min; RCY: 57–129 MBq (3–5%, d.c.); RCP: > 98%; A_m = 11.6 ± 3.4 GBq/µmol.

Biological characterization

In vitro stability assay: The in vitro stability was investigated using rat plasma. Thus, purified **[^{18}F]2** or **[^{18}F]3** was diluted in 200 µL E153 infusion solution and then incubated with 3 mL of rat plasma for 120 min at 37°C. Samples were taken after time points of 1, 30, 60 and 120 min, spotted on TLC plates and run (eluent: chloroform:methanol 9:1).

Generation of EphA2- and EphB4-transgenic A375 cells: Human A375 melanoma cells overexpressing EphA2 or EphB4 were prepared as described previously by us. [37, 40] In brief, A375 cells were stably transfected with a plasmid encoding both the reporter green fluorescent protein (GFP) and the EphA2 (A375-EphA2) or EphB4 receptor (A375-EphB4). GFP expression was used to select transfected cells by fluorescence associated cell sorting (FACS) and to routinely control stable expression of EphA2 and EphB4.

Verification of EphA2 and EphB4 overexpression: Enhanced EphA2 and EphB4 expression in A375-EphA2 and A375-EphB4 cells, respectively, was verified by western blotting as described previously.[37, 40]

Cellular binding and uptake studies and blocking experiments: Cellular binding and uptake of the radiotracers **[^{18}F]2** and **[^{18}F]3** were investigated in A375, A375-EphA2, and A375-EphB4 cells for up to 120 min as previously described by us.[37] For blocking experiments, cellular binding and uptake of **[^{18}F]2** and **[^{18}F]3** was investigated after pre-incubation with compound **2** for 30 min and lead compound **1** for 10 min, respectively. Cellular binding and uptake was investigated in at least two independent experiments, each performed in quadruplicate.

Acknowledgements

The authors are grateful to Jaques Pliquett, Waldemar Herzog, Stephan Preusche, and Tilow Krauss for their excellent technical and laboratory assistance. We are very thankful to Andrea

Suhr and Regina Herrlich for the in vitro and in vivo experiments. This work is part of a research initiative within the Helmholtz-Portfoliothema “Technologie und Medizin – Multimodale Bildgebung zur Aufklärung des In-vivo-Verhaltens von polymeren Biomaterialien”.

References

1. Mosch, B., et al., *Eph receptors and ephrin ligands: important players in angiogenesis and tumor angiogenesis.* Journal of Oncology, 2010. **2010**: p. 135285.
2. Liang, L.Y., et al., *Eph receptor signalling: from catalytic to non-catalytic functions.* Oncogene, 2019. **38**(39): p. 6567-6584.
3. Flanagan, J.G. and P. Vanderhaeghen, *The ephrins and Eph receptors in neural development.* Annual Review of Neuroscience, 1998. **21**: p. 309-345.
4. Cheng, N., D.M. Brantley, and J. Chen, *The ephrins and Eph receptors in angiogenesis.* Cytokine & Growth Factor Reviews, 2002. **13**(1): p. 75-85.
5. Pasquale, E.B., *Eph-ephrin bidirectional signaling in physiology and disease.* Cell, 2008. **133**(1): p. 38-52.
6. Zhao, C., et al., *Bidirectional ephrinB2-EphB4 signaling controls bone homeostasis.* Cell Metabolism, 2006. **4**(2): p. 111-121.
7. Pasquale, E.B., *Eph receptor signalling casts a wide net on cell behaviour.* Nature Reviews Molecular Cell Biology, 2005. **6**(6): p. 462-75.
8. Chen, J., *Regulation of tumor initiation and metastatic progression by Eph receptor tyrosine kinases.* Advances in cancer research 2012. **114**: p. 1-20.
9. Pasquale, E.B. and N.K. Noren, *Paradoxes of the EphB4 receptor in cancer.* Cancer Research, 2007. **67**(9): p. 3994-3997.
10. Lisle, J.E., et al., *Eph receptors and their ligands: promising molecular biomarkers and therapeutic targets in prostate cancer.* Biochim Biophys Acta, 2013. **1835**(2): p. 243-57.
11. Yang, X.K., et al., *EphB4 inhibitor overcome the acquired resistance to cisplatin in melanomas xenograft model.* Journal of Pharmacological Sciences, 2015. **129**(1): p. 65-71.
12. Guijarro-Munoz, I., et al., *Gene expression profiling identifies EPHB4 as a potential predictive biomarker in colorectal cancer patients treated with bevacizumab.* Medical Oncology, 2013. **30**(2).
13. Koolpe, M., M. Dail, and E.B. Pasquale, *An ephrin mimetic peptide that selectively targets the EphA2 receptor.* Journal of Biological Chemistry, 2002. **277**(49): p. 46974-46979.
14. Chrencik, J.E., et al., *Three-dimensional structure of the EphB2 receptor in complex with an antagonistic peptide reveals a novel mode of inhibition.* Journal of Biological Chemistry, 2007. **282**(50): p. 36505-36513.
15. Ma, B.Y., et al., *Investigation of the interactions between the EphB2 receptor and SNEW peptide variants.* Growth Factors, 2014. **32**(6): p. 236-246.
16. Noberini, R., I. Lamberto, and E.B. Pasquale, *Targeting Eph receptors with peptides and small molecules: Progress and challenges.* Seminars in Cell & Developmental Biology, 2012. **23**(1): p. 51-57.
17. Liu, Y., et al., *(99m)Tc-labeled SWL specific peptide for targeting EphA2 receptor.* Nucl Med Biol, 2014. **41**(6): p. 450-6.
18. Xiong, C.Y., et al., *In Vivo Small-Animal PET/CT of EphB4 Receptors Using Cu-64-Labeled Peptide.* Journal of Nuclear Medicine, 2011. **52**(2): p. 241-248.
19. Pretze, M., et al., *An Efficient Bioorthogonal Strategy Using CuAAC Click Chemistry for Radiofluorinations of SNEW Peptides and the Role of Copper Depletion.* ChemMedChem, 2013. **8**(6): p. 935-945.
20. Pretze, M., et al., *Radiofluorination and first radiopharmacological characterization of a SWLAY peptide-based ligand targeting EphA2.* Journal of Labelled Compounds & Radiopharmaceuticals, 2014. **57**(11): p. 660-665.
21. Ebert, K., et al., *Development of indazolylpyrimidine derivatives as high-affine EphB4 receptor ligands and potential PET radiotracers.* Bioorganic & Medicinal Chemistry, 2015. **23**(17): p. 6025-6035.
22. Mamat, C., et al., *Fluorine-18 Radiolabeling and Radiopharmacological Characterization of a Benzodioxolylpyrimidine-based Radiotracer Targeting the Receptor Tyrosine Kinase EphB4.* Chemmedchem, 2012. **7**(11): p. 1991-2003.

23. Wiemer, J., et al., *Preparation of a novel radiotracer targeting the EphB4 receptor via radiofluorination using spiro azetidinium salts as precursor.* Journal of Labelled Compounds & Radiopharmaceuticals, 2017. **60**(10): p. 489-498.
24. Lafleur, K., et al., *Structure based optimization of potent and selective inhibitors of the tyrosine kinase erythropoietin producing human hepatocellular carcinoma receptor B4 (EphB4).* Journal of Medicinal Chemistry, 2009. **52**(20): p. 6433-6446.
25. Lafleur, K., et al., *Optimization of Inhibitors of the Tyrosine Kinase EphB4. 2. Cellular Potency Improvement and Binding Mode Validation by X-ray Crystallography.* Journal of Medicinal Chemistry, 2013. **56**(1): p. 84-96.
26. Pretze, M., D. Pietzsch, and C. Mamat, *Recent Trends in Bioorthogonal Click-Radiolabeling Reactions Using Fluorine-18.* Molecules, 2013. **18**(7): p. 8618-8665.
27. Traxler, P. and P. Furet, *Strategies toward the design of novel and selective protein tyrosine kinase inhibitors.* Pharmacol Ther, 1999. **82**(2-3): p. 195-206.
28. Kirmse, W.S., H.J.; Bücking, H.-W. , *Reaktionen γ-substituierter Alkylcarbene.* Chem. Ber., 1966. **99**: p. 2579-2592.
29. Traube, W., *Der synthetische Aufbau der Harnsäure, des Xanthins, Theobromins, Theophyllins und Caffeïns aus der Cyanessigsäure.* Berichte der deutschen chemischen Gesellschaft, 1900. **33**(3): p. 3035-3056.
30. ~~ww.ccdc.cam.ac.uk/data_request/cif., C.x.c.t.s.c.d.f.t.p.T.d.c.b.o.f.o.c.f.t.C.C.D.C.v.~~
31. Kinski, E., *Master thesis.* 2012.
32. Pretze, M., PhD thesis, 2014.
33. ChemDraw Professional, V., PerkinElmer Informatics.
34. ACD Labs, V.x.
35. Cai, L.S., S.Y. Lu, and V.W. Pike, *Chemistry with [F-18]fluoride ion.* European Journal of Organic Chemistry, 2008(17): p. 2853-2873.
36. Hicks, J.W., et al., *Radiolabeled small molecule protein kinase inhibitors for imaging with PET or SPECT.* Molecules, 2010. **15**(11): p. 8260-78.
37. Mamat, C., et al., *Fluorine-18 Radiolabeling and Radiopharmacological Characterization of a Benzodioxolylpyrimidine-based Radiotracer Targeting the Receptor Tyrosine Kinase EphB4.* Chemmedchem, 2012. **7**(11): p. 1991-2003.
38. van Muijlwijk-Koezen, J.E., et al., *Synthesis and use of FSCPX, an irreversible adenosine A(1) antagonist, as a 'receptor knock-down' tool.* Bioorganic & Medicinal Chemistry Letters, 2001. **11**(6): p. 815-818.
39. a) G. M. Sheldrick, S.-a.S.-., Programs for the Solution and Refinement of Crystal Structures, University of Göttingen, 1997; b) G. M. Sheldrick, Acta. Cryst. 2008, A64, 112-122.
40. Mosch, B., D. Pietzsch, and J. Pietzsch, *Irradiation affects cellular properties and Eph receptor expression in human melanoma cells.* Cell adhesion & migration 2012. **6**(2): p. 113-25.